

Quaternary $\text{Cu}_2\text{ZnSnSe}_4$ Thin Films for Solar Cells Applications

G. Zoppi^{1*}, I. Forbes¹, R. W. Miles¹, P. J. Dale^{2†}, J. J. Scragg and L. M. Peter²

¹Northumbria Photovoltaics Applications Centre, Northumbria University, Ellison Building, Newcastle upon Tyne, NE1 8ST, UK

²Department of Chemistry, University of Bath, Bath, BA2 7AY, UK

[†] Now at Laboratoire Photovoltaïque, Université du Luxembourg, c/o CRP - Gabriel

Lippmann, 41, rue du Brill, L-4422 Belvaux, Luxembourg

Corresponding Author: guillaume.zoppi@northumbria.ac.uk

Abstract

Polycrystalline thin films of $\text{Cu}_2\text{ZnSnSe}_4$ (CZTSe) were produced by selenisation of $\text{Cu}(\text{Zn},\text{Sn})$ magnetron sputtered metallic precursors for solar cell applications. The p-type CZTSe absorber films were found to crystallize in the stannite structure ($a = 5.684 \text{ \AA}$ and $c = 11.353 \text{ \AA}$) with an electronic bandgap of 0.9 eV. Solar cells with the structure were fabricated with device efficiencies up to 3.2%.

1. Introduction

Thin film of $\text{Cu}_2\text{ZnSnS}_4$ (CZTS) and $\text{Cu}_2\text{ZnSnSe}_4$ (CZTSe) have attracted significant interest lately as alternative absorber layers in $\text{Cu}(\text{In},\text{Ga})(\text{S},\text{Se})_2$ (CIGS) thin film solar cells. Both CZTS and CZTSe are direct bandgap semiconductors with high absorption coefficient (10^4 cm^{-1}) [1]. This type of absorber derives from the CuInSe_2 chalcopyrite structure by substituting half of the indium atoms with zinc and the other half with tin. The resulting energy bandgap of this material has been reported to range from 0.8 eV for the selenide to 1.5 eV for the sulfide [2, 3] and devices based on CZTS have been made with efficiencies up to 6.7% [4]. Only limited studies have been done on CZTSe and devices have been reported on only two occasions [2, 5].

In this work, CZTSe films were produced by sequential deposition of high purity sputtered Cu, Zn and Sn from elemental targets followed by selenisation at high temperature. We report on some of the absorber properties and device results.

2. Experimental

CZTSe thin films were produced by a two stage process by means of selenisation of magnetron sputtered metallic $\text{Cu}(\text{Zn},\text{Sn})$ (CZT) precursor layers. The Cu, Zn and Sn layers were sequentially sputter

deposited using high purity (5N) targets onto unheated Mo coated soda-lime glass substrates on a rotating substrate table. The selenisation process took place in a mixed argon and elemental selenium atmosphere at temperatures of 500°C for 30 min. The thickness of the precursor was adjusted so that the final thickness of the CZTSe film was $\sim 2 \mu\text{m}$. Devices were made by the deposition of a 70 nm CdS window layer using the chemical bath deposition method, followed by the deposition of 50 nm i-ZnO and 400 nm indium tin oxide (ITO) using rf sputtering. The cells were finished using sputtered Ni/Al contacts.

The structural quality of the absorber layers was examined using X-ray diffraction (XRD) carried out with a Siemens D-5000 diffractometer using a $\text{CuK}\alpha$ radiation source ($\lambda = 1.5406 \text{ \AA}$). The film morphology and composition were determined using a FEI Quanta 200 scanning electron microscope (SEM) equipped with an Oxford Instruments energy dispersive X-ray analyzer (EDS). Depth profiling and investigations of lateral uniformity of the layers were investigated using a bench-top Millbrook MiniSIMS (secondary ion mass spectroscopy) system with a Ga^+ primary ion of 6 keV. Photocurrent spectra of the devices were recorded using a double grating monochromator with chopped illumination normalized against calibrated silicon and germanium photodiodes. Current - voltage measurements were recorded at 25°C under AM1.5 ($100 \text{ mW}\cdot\text{cm}^{-2}$) illumination. Reflectance measurements were recorded using a Shimadzu SolidSpec-3700.

3. Results & Discussion

The XRD pattern of a CZT precursor layer on Mo-coated glass is presented in figure 1, the corresponding composition data is shown in Table 1. The film was intentionally deposited Cu poor ($\text{Cu}/(\text{Zn}+\text{Sn}) = 0.85$), with approximately

equal amounts of Zn and Sn. Table 1 indicates that the film was slightly Sn poor (Zn/Sn = 1.08). XRD analysis of the precursor film revealed the presence of elemental Zn and Sn, but not Cu. Cu was found to be present in the form of binaries with Zn (Cu_5Zn_8) and Sn ($\eta\text{-Cu}_6\text{Sn}_5$) but there was no evidence of any Zn_xSn_y sub-phase formation during the deposition of the precursor. This is in agreement with Cu-Sn-Zn solder alloy studies which have shown that Zn and Sn react preferentially with Cu [6, 7]. After selenisation at 500°C for 30 min, EDS measurements indicated that the film conserves its overall Cu-poor and slightly Sn-poor composition (Table 1).

	CZT precursor	CZTSe absorber
Cu/(Zn+Sn)	0.85	0.83
Zn/Sn	1.08	1.15
Se/(Cu+Zn+Sn)	-	1.02

Table 1. Elemental composition of the CZT metallic precursor and subsequent selenised films at 500°C for 30 min.

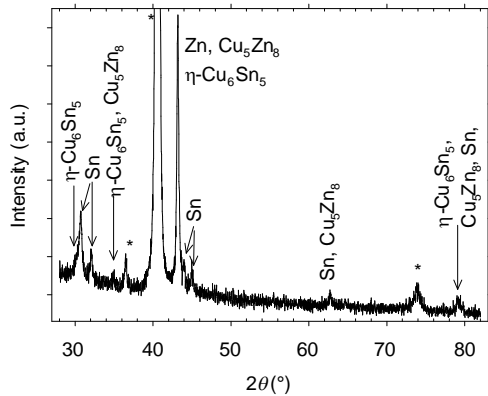


Figure 1. XRD pattern of a Cu(Zn,Sn) precursor film with Cu/(Zn+Sn)=0.85 and Zn/Sn=1.08 deposited on Mo-coated glass. Peaks marked (*) arise from the substrate.

Figure 2 shows the corresponding XRD pattern of a CZTSe film selenised at 500°C for 30 min. All the peaks can be attributed to $\text{Cu}_2\text{ZnSnSe}_4$. The calculated lattice parameters are $a = 5.684 \text{ \AA}$ and $c = 11.353 \text{ \AA}$, in very good agreement with the published data from Matsushita *et al.* [8] and Olekseyuk *et al.* [9]. The doublet peaks (312/116) and (400/008) are observed and together with the previous cited references this indicates that the selenised film adopts the stannite [I4-2M] structure. Figure 3 shows the morphology

of the 2 μm thick CZTSe film processed at 500°C. The film consists of closely packed grains which are $\sim 2 \mu\text{m}$ wide.

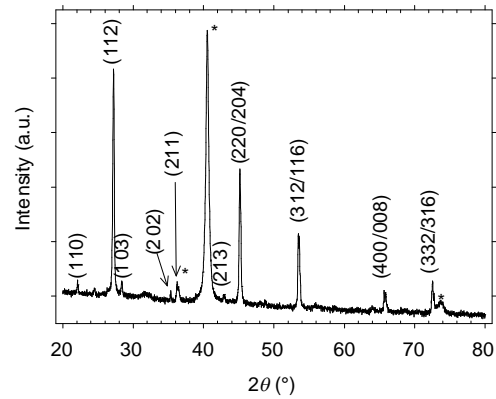


Figure 2. XRD pattern of a $\text{Cu}_2\text{ZnSnSe}_4$ (CZTSe) film selenised at 500°C for 30 min. Peaks marked (*) arise from the substrate, and all other peaks belong to the CZTSe structure.

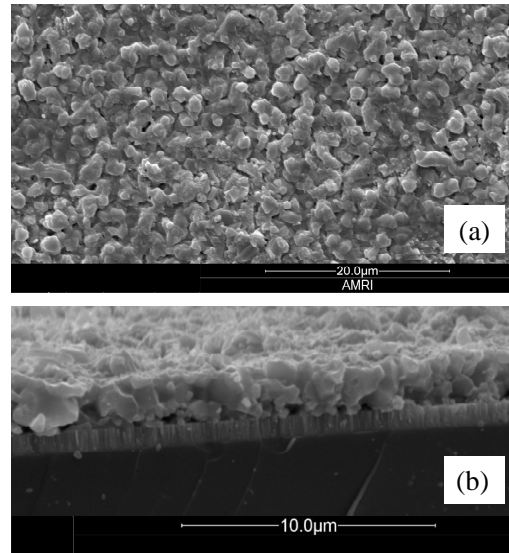


Figure 3. Scanning electron micrograph of a CZTSe film on Mo-coated glass. (a) Surface image and (b) cross-sectional image.

The elemental distribution of the films as a function of depth was probed by SIMS, and a depth profile of the four elements is shown in figure 4 for a sample selenised at 500°C. This qualitative assessment indicates a uniform distribution of the Se and Sn metallic elements throughout the film thickness. The Cu signal is also uniform for the majority of the film. However, the increase in the Cu signal towards the interface with the substrate is attributed to excess Cu deposited during the precursor preparation, to improve

adhesion to the substrate. Finally, the Zn profile appears to show a dip in the middle of the film. However, due to the low sensitivity for the Zn ions in the CZTSe matrix, further analysis is required to determine whether this is a real feature or this is due to the morphology of the film.

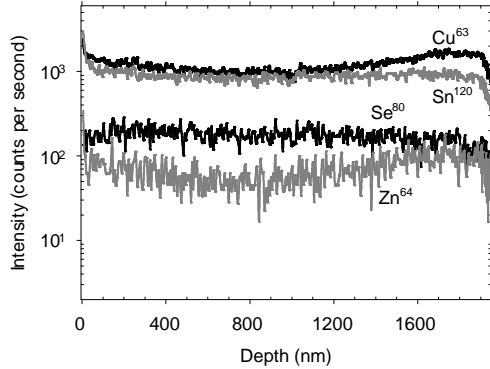


Figure 4. MiniSIMS depth profiles of a CZTSe film deposited on glass. The precursor was selenised at 500°C for 30 min.

Figure 5 shows the current density - voltage (J - V) curves for two selected devices under AM1.5 standard illumination and in the dark. The corresponding cell parameters are shown in Table 2. Cell A represents the device with the best fill factor (FF) of 0.48 while cell B is the solar cell with the best open circuit voltage (V_{oc}) of 0.359 V. This yields an efficiency of 3.0% and 3.2% for cell A and B, respectively for a total area of 0.229 cm².

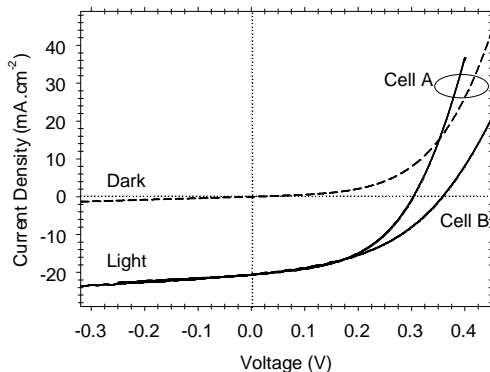


Figure 5. Dark and light current density - voltage curves of the best performing CZTSe solar cells recorded under AM1.5 (100 mW.cm⁻², 25°C) illumination and total device area of 0.229 cm².

The efficiency is limited partly by the fill factor indicated by the high shunt conductance (G_{sh}) (8.0 and 9.1 mS.cm⁻² for cell A and B, respectively) and high series resistance (R_s) (2.2 and 3.9 Ω.cm²

for cell A and B, respectively). The J - V measurements also showed a crossover of the dark and light current voltage curve (figure 5, cell A) that is characteristic of large series resistance. Due to a non-optimum grid design, an estimated 20% of the total area is covered by the grid and as a comparison, this would yield efficiencies of 3.6% and 4.0% for cells A and B, respectively for an active area of 0.184 cm². This constitutes a significant improvement when compared to Friedmeier *et al*'s 0.8% device [2] and Altosaar *et al*'s 1.8% monograin structure [5].

	V_{oc} (V)	J_{sc} (mA.cm ⁻²)	FF	η (%)
Cell A	0.304	20.6	0.48	3.0
Cell B	0.359	20.7	0.43	3.2

Table 2. Solar cells parameters. The definition of symbols is given in the text.

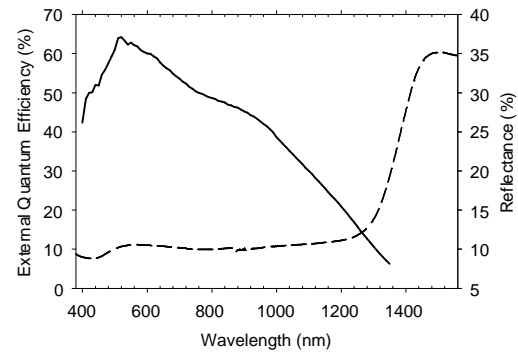


Figure 6. External quantum efficiency (EQE) for a CZTSe solar cell (Cell B) (solid line) and reflectance data for a CZTSe film (dashed line).

Figure 6 shows the external quantum efficiency (EQE) for cell B. The maximum quantum efficiency of 65% is obtained for a photon wavelength of 520 nm and exhibits the characteristic short wavelength cut-off from the CdS buffer layer. The CZTSe devices are characterized by a long end tail curve sloping gradually from 520 nm which may be attributed to high doping densities and small electron diffusion length. The energy bandgap of the CZTSe film was extrapolated and found to be 0.94±0.05 eV. This is in agreement with our reflectance data, also plotted in figure 6, which shows the main optical transition to be at 0.88±0.04 eV. Friedmeier *et al.* estimated that their evaporated CZTSe

absorber thin films to have an energy bandgap of about 0.8 eV [2]. The spread observed in bandgap values could be due to differences in stoichiometry but also to the presence of additional phases.

The *EQE* spectrum measured under zero voltage bias, figure 6, was also used to calculate the expected short circuit current density (J_{sc}). The value of J_{sc} calculated by integrating the *EQE* response with the AM1.5 solar spectrum is 19.7 mA.cm⁻² which is in close agreement with the measured value from the *J-V* curve (20.7 mA.cm⁻²). The difference arises due to missing *EQE* data at long wavelength.

4. Conclusion

It has been shown that good quality Cu₂ZnSnSe₄ (CZTSe) material can be produced for solar cell applications using a 2-stage sputtering-selenisation process. The slightly Cu-poor and Zn-rich absorbers showed good optical and electronic properties and were successfully made into solar cells achieving efficiency of 3.2%. To the authors' best knowledge this is the highest reported efficiency for a device based on a Cu₂ZnSnSe₄ absorber. These devices are currently limited by the current generation and collection as indicated by spectral response and current-voltage measurements.

Acknowledgments

This work was funded by the EPSRC SUPERGEN programme "Photovoltaics for the 21st Century".

References

- [1] K. Ito and T. Nakazawa, Japanese Journal of Applied Physics **27** (1988) 2094-2097
- [2] T. M. Friedlmeier, N. Wieser, T. Walter, H. Dittrich, and H. W. Schock, Proceedings of the 14th European Photovoltaic Specialists Conference, Barcelona (1997) 1242-1245
- [3] H. Katagiri, Thin Solid Films **480-481** (2005) 426-432
- [4] H. Katagiri, K. Jimbo, S. Yamada, T. Kamimura, W. S. Maw, T. Fukano, T. Ito, and T. Motohiro, Applied Physics Express **1** (2008) 041201
- [5] M. Altosaar, J. Raudoja, K. Timmo, M. Danilson, M. Grossberg, M. Krunk, T. Varema, and E. Mellikov, Proceedings of

the 4th IEEE World Conference on Photovoltaic Energy Conversion, (2006) 468-470

[6] M.-C. Wang, S.-P. Yu, T.-C. Chang, and M.-H. Hon, Journal of Alloys and Compounds **381** (2004) 162-167

[7] T. Ichitsubo, E. Matsubara, K. Fujiwara, M. Yamaguchi, H. Irie, S. Kumamoto, and T. Anada, Journal of Alloys and Compounds **392** (2005) 200-205

[8] H. Matsushita, T. Maeda, A. Katsui, and T. Takizawa, Journal of Crystal Growth **208** (2000) 416-422

[9] I. D. Olekseyuk, L. D. Gulay, I. V. Dydchak, L. V. Piskach, O. V. Parasyuk, and O. V. Marchuk, Journal of Alloys and Compounds **340** (2002) 141-145